Seismic Behavior of Historical Masonry Bridges: The Case Study of Irgandi Bridge

Gökhan Barış Sakcalı[1,*], Alper Gönül[2] and İsa Yüksel[1]

[1]*Department of Civil Engineering, Bursa Technical University, Bursa, Turkey*

[2]*Department of Architecture, Bursa Technical University, Bursa, Turkey*

Abstract: In Anatolia, numerous bridges have been constructed throughout history for essential reasons. It is important to preserve the bridges and hand them down to the future generations as they have hints regarding the materials and construction techniques used in the past. Irgandi Bridge located on Gökdere in Bursa city, which is the first capital of Ottoman Empire, has a special importance among bridges around the world. It is one of the few bridges around the world, which have had commercial activities with shops on it along with the purpose of transportation. This symbolic structure in terms of cultural, historical and constructional aspects is located in Bursa which includes 1st degree seismic hazard zone. Therefore, preservation of the bridge requires investigation of its seismic performance and taking necessary precautions. Irgandi Bridge was modeled by ANSYS software using finite element method (FEM). Convergence study was performed to determine the accurate number of elements. Modal and linear dynamic analysis of the Irgandi Bridge was conducted after the number of elements were determined by the convergence study. Therefore, seven earthquake records were scaled and performed to the system according to EC-8 (Eurocode-8). Stress distributions and displacements were examined as a result of linear dynamic analysis. It was determined that the maximum displacement occurred at the top of the bridge and the principal stress occurred in the support regions. As a result of the analyses, it was proposed to strengthen the support parts of the bridge, which were determined to be damaged under earthquake impact.

Keywords: Finite Element Method, Historic Bridges, Irgandi Bridge, Linear Dynamic Analysis.

1. INTRODUCTION

Irgandi Bridge, located in Gökdere, in the city center of Bursa, was built in 1442 during the reign of sixth Ottoman Sultan - Murad II. Irgandi Bridge, which was one of the four bridges with bazaars in the world, contained 32 shops when it was first built, but now there are 16 shops on it. Irgandi Bridge, built as stone masonry, was destroyed during the War of Independence. In 1949, the bridge was rebuilt using unreinforced concrete in the arch; limestone and lime mortar in the spandrel walls.

Modeling and analysis of historical masonry arch bridges date back to the 1970s. In the early 1970s, 1D (one-dimensional) modeling approach was first used. However, it has been concluded that this method does not show a realistic stress distribution as it consist of cracks in the structure under service loads [1]. Therefore, the 2D (two-dimensional) modeling approach, which is more realistic than the 1D modeling approach, began to be used in the following years. While this modeling approach obtained much more realistic results than the 1D modeling approach, it did not obtain realistic results in determining the collapse mechanism in asymmetrical bridges and arches [2].

Finally, 3D (three dimensional) modeling approach has been used as a more realistic modeling method.

Three different modeling methods are used in the modeling of masonry structures (Figure **1**) [3]. In micro modeling method, stone or brick material or mortar material is modeled independent of each other (Figure **1a**). In this modeling method, the system behavior is reflected quite realistically as the mechanical properties of materials are defined independently and precisely. However, in large scale and 3D structures, this type of modeling requires large computational capability and time. Instead of this modeling technique, simplified micro modeling technique has been developed. In this method, an interface is defined between two stone or brick materials (Figure **1b**). This modeling method requires less computational capability and time than detailed micro modeling technique, but requires large computational capability and time in complex and gigantic structures. For this reason, macro modeling method is preferred in studies evaluating the whole structure (Figure **1c**). When the mechanical properties and boundary conditions of materials are correctly defined, it has been proven by experimental studies that the macro model gives results as close to reality as the micro model. In addition, the macro modeling technique significantly reduces the analysis time of the modeling method [4]. In this study, macro modeling method was used to shorten the analysis time.

*Address correspondence to this author at the Department of Civil Engineering, Bursa Technical University Faculty of Engineering and Natural Sciences, Bursa, Turkey; Tel: +90224 300 3512; Fax: +90224 300 3419; E-mail: gokhan.sakcali@btu.edu.tr
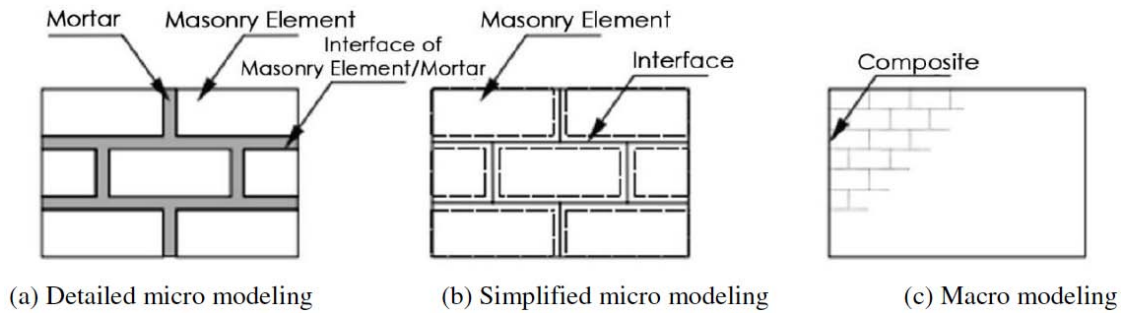
Figure 1: Modeling methods for masonry structures [3].

Masonry structures are often modeled by discrete or finite element method. As part of this study, the Irgandi Bridge, a masonry structure, is modeled with the finite element method. This method turns a structural or non-structural physical system into a mathematical equation, giving the approximate solution of the system. When using this method, analysis type, material properties, model geometry, boundary conditions and loads as well as a realistic definition of element type and correct selection of the number of element is of great importance in the realistic outcome of the analysis.

$$[K][D]+[M][\ddot{D}] = 0 \qquad (1)$$

$$[K][D]+[C][\dot{D}]+[M][\ddot{D}] = [R] \qquad (2)$$

In the finite element method, Equation 1 was used for modal analysis and Equation 2 was used for dynamic analysis [5]. Since the Equation 1 is used for modal analysis and these analyses are independent from external loads on the system, the right side of the Equation 1 was given as zero. K refers to the global stiffness matrix generated by the geometric properties of the element or system, C refers to the matrix of damping coefficient, R refers to a vector of all the equivalent nodal force vectors, M refers to the mass matrix and D refers to a vector of all displacements at all the nodes in the entire problem domain. Depending on the displacements obtained, the desired data such as stresses could be easily found in the system. Modeling the Irgandi Bridge with finite element method was made using Ansys [6] software. SOLID 65-type element was used in this software for the identification of brittle materials such as concrete, stone and brick.

2. METHOD OF ANALYSIS

2.1. Material Properties

Irgandi Bridge was consisted of a single arch, spandrel walls and backfill material. The arch was made up of unreinforced concrete, while the spandrel walls were made up of limestone and lime mortar. Core samples were taken from the arch structure of Irgandi Bridge as part of the restoration work conducted by Bursa Metropolitan Municipality in 2003 (Table **1**). The mean value (33.5 MPa) of these samples was used in the arch structure of the bridge consisting of unreinforced concrete. The Young's modulus was determined by putting this mean value of concrete compressive strength in the Equation 3 [7]. In Equation 3, E refers to the Young's modulus and f_c is the concrete compressive strength. The properties of concrete materials used in analysis are shown in Table **2**.

$$E = 4750\sqrt{f_C} \qquad (3)$$

Table 1:   Core Samples

Sample No	Compressive Strength (MPa)
1	34.0
2	40.0
3	23.9
4	40.2
5	35.8
6	31.8
7	27.8
8	34.5

Table 2:   Material Properties of the Arch

Density (kg/m³)	Poisson's ratio	Young's modulus (MPa)
2300	0.2	27493

In the scope of the study, the most critical values of the material properties given in the literature are used for limestone and lime mortar materials that were required for the construction of spandrel walls [8]. In

Equation (4), homogenized wall compressive strength could be obtained based on the compressive strengths of the materials used in the wall. In the Equation (4), f_b refers to the compressive strength of brick or stone, f_m refers to the compressive strength of the mortar and f_{mas} refers to the compressive strength of the homogenized masonry structure [9]. The Young's modulus of the homogenized wall was determined by Equation 5 [10]. The homogenized density and Poisson ratio of the spandrel wall could be calculated from Equations (6-7). In these equations; Y_{st}, Y_m and Y_{mas} refer to the densities of the stone, mortar, and the homogenized material, respectively. Similarly, v_{st}, v_m, and v_{mas} show Poisson ratio of stone, mortar, and the homogenized material, respectively. V_{st} is the volume of the stone or brick and V_m is the volume of the mortar [11]. The calculated values are given in Table **3**. In addition, the values given in the literature were used for backfill material properties and these values are shown in Table **4** [12].

$$f_{mas} = 0.6 f_b^{0.65} f_m^{0.25} \tag{4}$$

$$E_{mas} = 1000 f_{mas} \tag{5}$$

$$\gamma_{mas} = \gamma_{st} V_{st} + v_m V_m \tag{6}$$

$$v_{mas} = v_{st} V_{st} + v_m V_m \tag{7}$$

2.2. Loads

Figure **3** shows the side elevation and A-A cross section at the Irgandi Bridge. Within the scope of this study, dead loads of timber shops and pavement on the bridge acting on the unit area are determined. Loads of these shops were calculated according to the cross section given in Figure **2**. According to this section, density of Scotch Pine is 4.26 kN/m^3 (the shops on the bridge were constructed by using Scotch Pine). In addition, it was accepted that the density of mortar is 19 kN/m^3 and the unit roof load of the shops is 1.5 kN/m^2 [13]. The paving stones of the bridge are made of slate stone. The density of slate, backfill material and mortar were taken as 27 kN/m^3, 23 kN/m^3 and 19 kN/m^3, respectively. For multifunctional bridges that do not pass motor vehicles, 5 kN/m^2 can be used as the moving load value [14].

$$Load\ combination = 1.25 x DL + 1.35 x LL \tag{8}$$

The load combination was calculated considering the overload condition stated in Equation 8. In the

Table 3: Material Properties of Spandrel Walls and Backfill Material

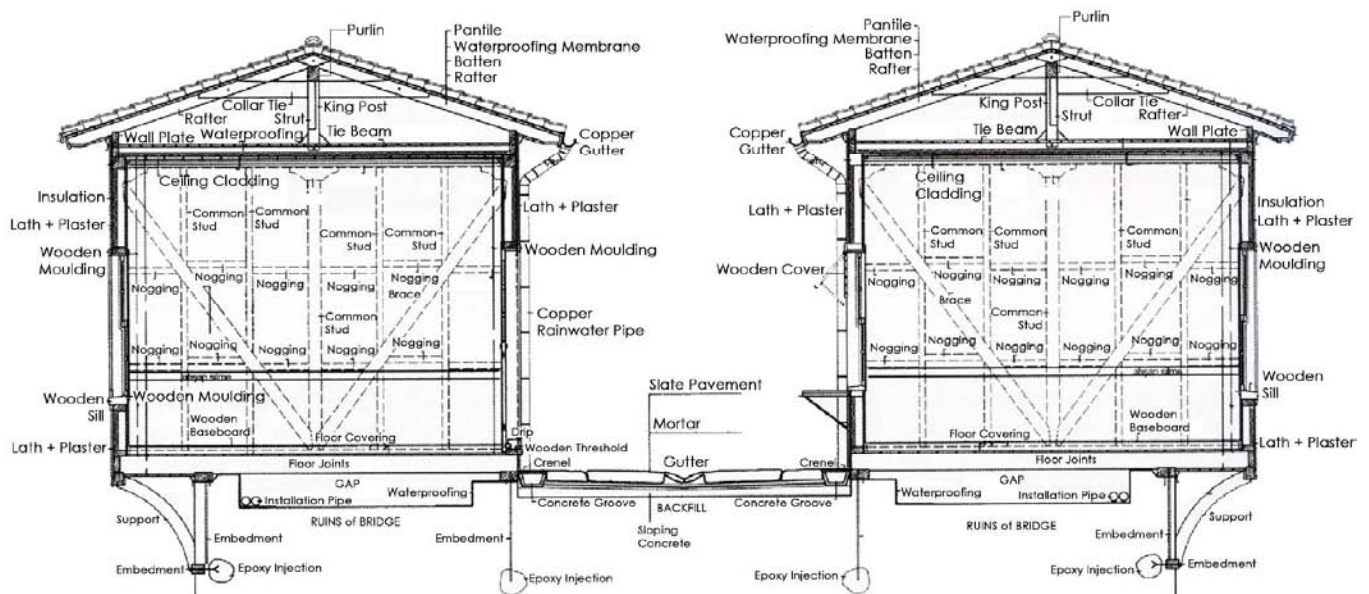| Element of structure	Density (kg/m^3)	Poisson ratio	Young's modulus (MPa)
Spandrel walls	2510	0.29	7518
Backfill material	1800	0.20	500

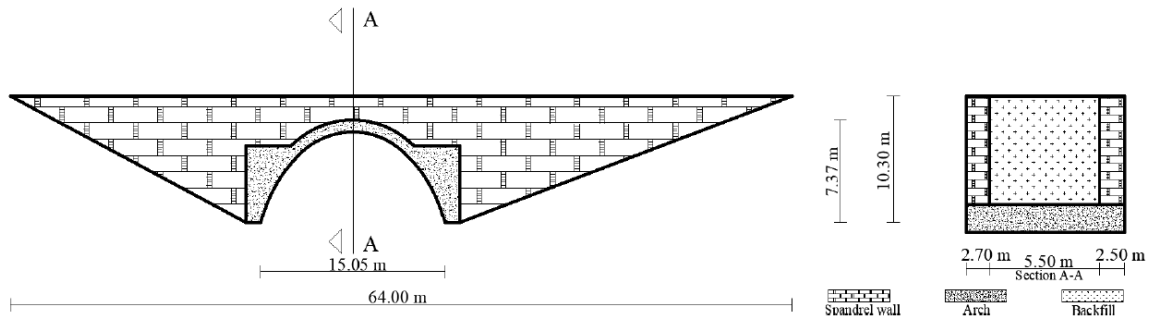**Figure 2:** Section of shops on Irgandi Bridge [15].

Figure 3: Side elevation and section of Irgandi Bridge.

Equation 8, DL refers to dead load of the structure; LL refers to live load of the structure. Additionally, it was assumed in analysis that the ground on which the building was located is completely rigid and there is no displacement in the supports of the bridge [14].

2.3. Analysis

In this study, linear dynamic analysis of Irgandi Bridge is performed and earthquake performance is examined. 3D modeling approach by finite element method was used in this analysis to achieve more realistic results in the bridge model. The ground type, where this bridge is located, is type B. The generated

finite element model of the Irgandi Bridge is shown in Figure **4**. Because of the convergence study in this model, it was determined that the ideal nodes and number of elements are 57673 and 38376, respectively. Earthquake records for ground type-B are given in Table **4**. In the Table **4**; M_w is moment magnitude, R is depth, V_s is shear wave velocity and PGA is peak ground acceleration. For these earthquake recordings, shear wave velocity is required to be between 360 m/s and 800 m/s.

Therefore, shear wave velocity was chosen in the range of 410 m/s and 760 m/s. Additionally, moment magnitudes of the selected earthquake records for the
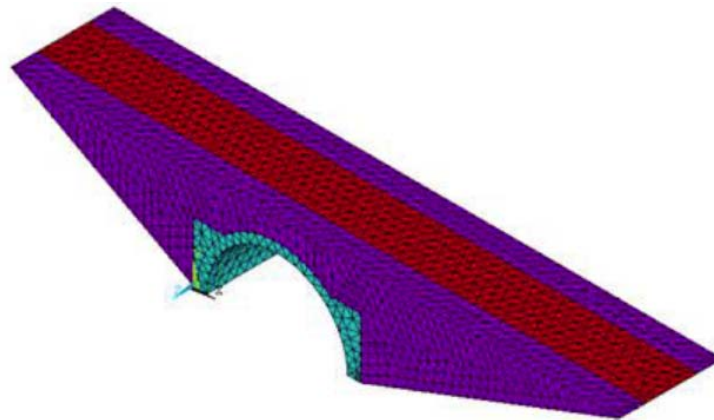

Figure 4: 3D Finite Element Model of Irgandi Bridge.

Table 4:   Selected Earthquake Records

Earthquake record	Station	Ground type	M_w	R (km)	V_s (m/s)	PGA (g)
Tabas, Iran	Tabas	B	7.35	2.05	767	1.57
Loma Prieta	Corralitos	B	6.93	3.85	462	1.73
Cape Mendocino	Cape Mendocino	B	7.01	6.96	568	2.18
Kobe, Japan	Nishi-Akashi	B	6.90	7.08	609	1.93
Chi-Chi, Taiwan	TCU68	B	7.62	0.32	487	1.07
Northridge-01	Symar- Olive View Med FF	B	6.69	5.30	441	1.84
Montenegro, Yugoslavia	Ulcinj-Hotel Albatros	B	7.10	4.35	410	1.50

analysis varied between 6.69 and 7.62; and the PGA ranged from 1.07g to 2.18g.

Table 5:   Scaling Factors for Earthquake Record

Earthquake	Scaling Factor
Tabas, Iran	0.33
Loma Prieta	0.72
Cape Mendocino	0.62
Kobe, Japan	0.72
Chi-Chi, Taiwan	0.64
Northridge-01	0.61
Montenegro, Yugoslavia	1.36

Earthquake records were scaled between 0.2T and T according to the design spectrum of Eurocode-8 [16]. The scaling factors are given in Table **5**. 5% damping ratio was used in this analysis. The spectra resulting from combining each earthquake record using SRSS (Square-Root-Sum-of-Squares) after scaling, and the design spectra drawn according to Eurocode-8 are shown in Figure **5**.
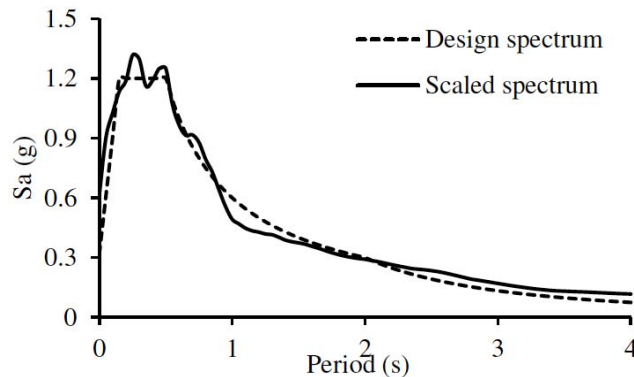

Figure 5: Design and scaled spectrum.

3. RESULTS AND DISCUSSIONS

3.1. Modal Analysis Results

Modes are inherent properties of a structure, and are determined by the structural properties such as mass, damping, and stiffness. Moreover, boundary conditions also affect modes of a structure. Each mode is defined by a natural frequency, modal damping and a mode shape. Modal analysis is a procedure that determines dynamic characteristics of a structure. It provides information about the characteristics of the structure by solving the situation when the load is not applied. Table **6** represents six natural frequencies and mode shapes of Irgandi Bridge. It can be observed that these six frequencies change in the range of 14.94 Hz-

25.81 Hz The first of the six vibration modes of the Irgandi Bridge is a bending mode that occurs in the direction parallel to river flow. Torsion is observed in the second, third and fifth vibration modes of the Irgandi Bridge and the frequencies of these modes are 17.28 Hz, 21.03 Hz and 25.25 Hz, respectively. Furthermore, the fourth mode of the Irgandi Bridge consists of the bending mode for the direction perpendicular to the river flow and the sixth mode consists of the vertical asymmetric mode. The frequencies in these modes are 21.10 Hz and 25.81 Hz, respectively. Besides, ratio effective mass to total mass corresponding to the mode shapes were examined in Irgandi Bridge. Ratio effective mass to total mass in the direction parallel to river flow was greater in the first mode than in the other models.
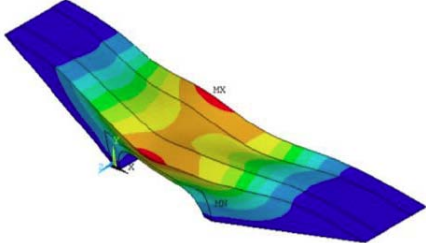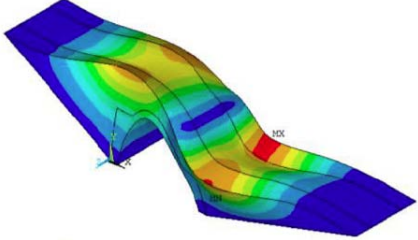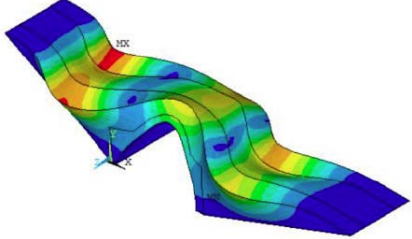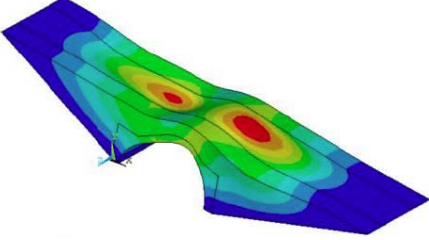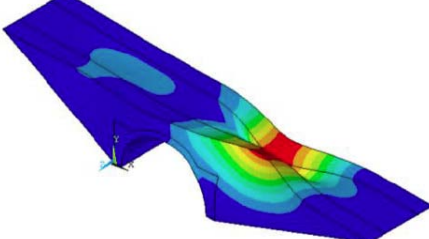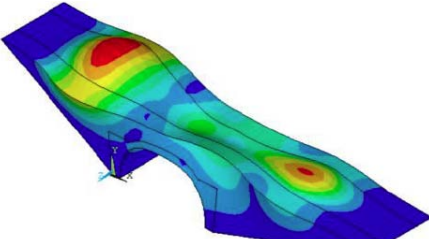
3.2. Linear Dynamic Analysis

3.2.1. Displacements

Linear dynamic analyses were performed using seven different earthquake records in order to determine the seismic performance of the Irgandi Bridge. Newmark method was used as the solution algorithm in linear dynamic analysis. In addition, Rayleigh damping coefficient was considered as 5% in linear dynamic analysis.

Displacement contours of the Irgandi Bridge both in the direction to the river flow and in the direction parallel to the river flow for Northridge-01 earthquake record are given in Figure **6a** and **6b**, respectively. Displacement contours are similar for other earthquake records. The maximum displacements in the direction perpendicular to the river flow of the bridge occur in the upper regions of the bridge, but maximum displacement is observed in two different regions of the bridge for all earthquake recordings (Figure **6a**). In addition, the maximum displacements of the bridge in the direction parallel to the river flow occur in the middle and upper regions of the bridge for all earthquake recordings (Figure **6b**). The maximum displacements of the bridge in the direction perpendicular to the river flow vary between 0.22 mm-0.90 mm while the maximum displacements of the bridge in the direction parallel to the river flow vary between 0.25 mm-1.75 mm as a result of the linear dynamic analyses performed for 7 different earthquake recordings (Table **6**). The averages of displacements of the bridge in these earthquake records for both directions are 0.48 mm and 0.99 mm, respectively. The average of the maximum displacements of the bridge in the direction parallel to the river flow is about 51.5%

Table 6: Frequencies and Mode Shapes of Irgandi Bridge

Mode	Mode shape	Behavior	Frequency (Hz)
1		1st bending mode for direction parallel to the river flow	14.94
2		1st torsional asymmetric mode	17.28
3		1st torsional symmetric mode	21.03
4		1st bending mode for direction perpendicular to the river flow	21.10
5		2nd torsional asymmetric mode	25.25
6		1st vertical asymmetric mode	25.81

(a) Direction perpendicular to the river flow
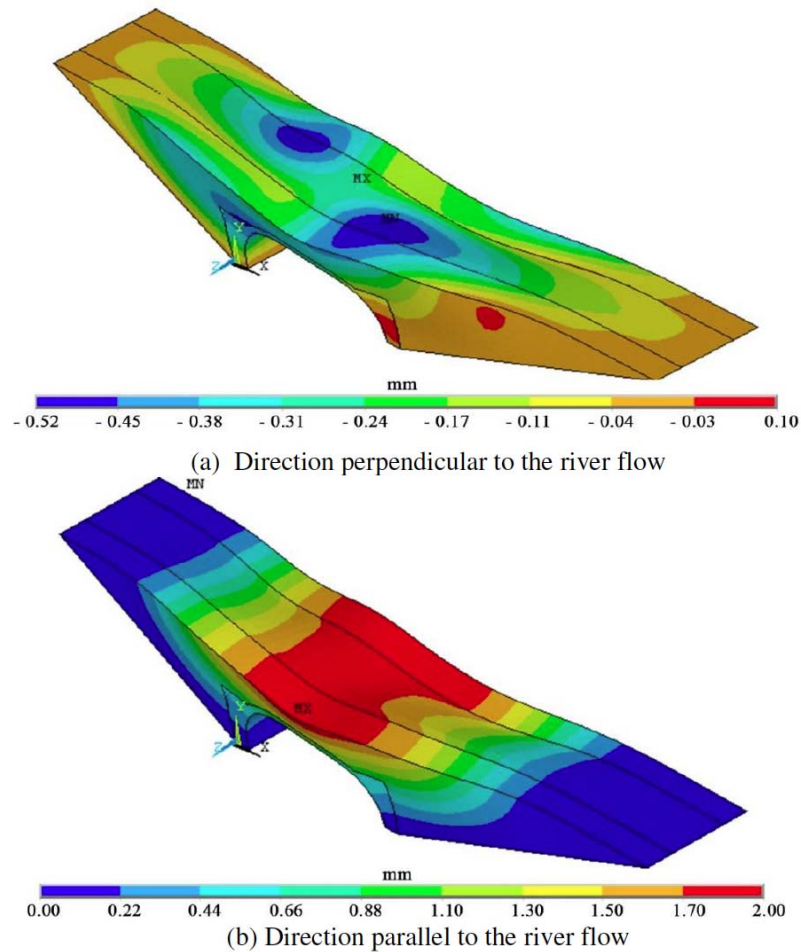

(b) Direction parallel to the river flow

Figure 6: Displacement contours of the bridge for Northridge-01 earthquake record.

Table 7:   Maximum Displacements for all Earthquake Records

Number	Earthquake record	Direction perpendicular to the river flow direction		Direction parallel to the river flow direction	
		Time (s)	Maximum displacement (mm)	Time (s)	Maximum displacement (mm)
1	Tabas	2.80	0.73	3.03	1.05
2	Loma Prieta	4.07	0.25	2.61	0.73
3	Cape Mendocino	4.07	0.26	2.61	0.60
4	Kobe	1.60	0.57	3.56	1.13
5	Chi-Chi	15.39	0.22	15.23	0.25
6	Northridge-01	1.02	0.46	1.06	1.75
7	Montenegro	4.18	0.90	3.79	1.40

higher than the average of the maximum displacements in the other direction.

3.2.2. Stresses

Maximum and minimum principal stress contours of Irgandi Bridge for Tabas earthquake record are given in Figure **7**. Maximum and minimum contours are similar for other earthquake records. It can be observed that both the maximum and the minimum principal stresses occur in the support zones of the arch of the Irgandi Bridge. The maximum values of these stresses for 7 different earthquake records are given in Table **8**.
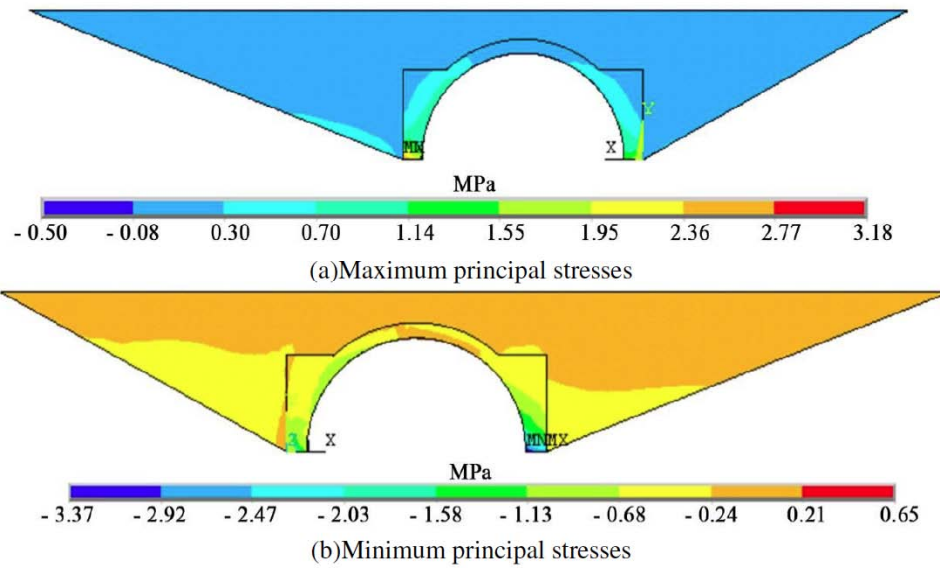
(a)Maximum principal stresses

(b)Minimum principal stresses

Figure 7: Maximum of maximum and minimum principal stress contours of the bridge for Tabas earthquake record.

Table 8: Maximum of Maximum and Minimum Principal Stress for all Earthquake Records

Number	Earthquake record	Time (s)	Max. principal stress (MPa)		Time (s)	Min. principal stress (MPa)	
			Arch	Spandrel wall		Arch	Spandrel wall
1	Tabas	3.66	3.00	0.53	2.93	3.05	0.33
2	Loma Prieta	2.61	3.57	0.55	2.61	3.77	1.26
3	Cape Mendocino	3.06	2.27	0.48	3.06	1.94	0.48
4	Kobe	3.56	5.03	1.35	5.08	1.93	0.51
5	Chi-Chi	15.24	2.61	0.77	28.65	1.00	0.34
6	Northridge-01	1.02	8.20	1.24	1.02	1.21	0.89
7	Montenegro	2.44	4.45	0.14	1.93	0.93	0.08

Maximum principal stresses vary between 2.27 MPa-8.20 MPa in the arch and 0.14-1.35 MPa in spandrel walls as a result of the linear dynamic analyses performed for 7 different earthquake recordings. For minimum principal stresses, these values range between 0.93 MPa-3.77 MPa and 0.08 MPa-1.26 MPa, respectively (Table **8**). The averages of maximum principal stresses in the Irgandi Bridge are 4.17 MPa in the arch and 0.7 MPa in the spandrel wall for all earthquake recordings. In addition, the averages of the minimum principal stresses for the arch and the spandrel wall are 1.97 MPa and 0.55 MPa, respectively.

Arch of Irgandi Bridge consists of unreinforced concrete and the spandrel wall of Irgandi Bridge is composed of limestone and lime mortar. The compressive strength of unreinforced concrete is 33.5 MPa, homogenized compressive strength of lime mortar and limestone is 7.51 MPa. The tensile strength

of these materials can be taken as 10% of the compressive strength. Damages to brittle materials were usually caused by tensile stresses. Therefore, the average of maximum strength occurring in the bridge and material tensile strength were compared. While the average of the maximum stresses occurring in the arch of Irgandi Bridge is 4.17 MPa, the tensile strength of the material is 3.35 MPa. This indicates that the arch of the Irgandi Bridge may be damaged. Potential damage to the arch is expected to occur near the support. In addition, while the average of the maximum stresses on the spandrel wall of the Irgandi Bridge is 0.7 MPa, the homogenized tensile strength of the spandrel wall material is 0.75 MPa. This indicates that the spandrel wall is unlikely to be damaged.

4. CONCLUSION

Recently, the preservation and restoration of historical structures is getting extremely importance.

Therefore, the behavior of historical structures under earthquake loads should be known. Thus, the structures could be strengthened without damaging the original features. In this study, earthquake behavior of historical Irgandi Bridge was investigated. Therefore, seven different earthquake records were scaled according to Eurocode-8. Each earthquake records were applied to the Irgandi Bridge, which has a finite element model, for linear dynamic analysis. As a result of analysis; it was observed that the displacement which occurs in the direction perpendicular to the river flow was more than the other direction. In addition, it was observed that maximum and minimum principal stresses occur in the Irgandi Bridge. It was seen that these stresses were maximum in the support zones of the bridge. This indicates that the damage to the Irgandi Bridge will occur primarily in the support zones in a possible earthquake. In this context, it is recommended to strengthen the support zones of this structure.

REFERENCES

[1]   Rouf MA. Fundamental properties of brickwork with particular emphasis to brickwork arches. Diss. University of Liverpool 1984.

[2]   Zhang Y. Advanced nonlinear analysis of masonry arch bridges. Diss. Imperial College London 2014.

[3]   Lourenço PB. Computational strategies for masonry structures. Diss. Delft University of Technology 1996.

[4]   Lourenço PB. Current experimental and numerical issues in masonry research. In: Lourenço PB, Barros JO, Oliveira DV, editor. 6º Congresso Nacional de Sismologia e Engenharia Sísmica. Guimarães - Portugal 2004. Universidade do Minho 2004; pp. 119-136.

[5]   Liu GR, Quek SS, The finite element method: A practical course, 2nd ed. Butterworth-Heinemann an imprint of Elsevier Science Linacre House: Oxford 2013.

[6]   ANSYS. Swanson Analysis System, Ansys Inc, Canonsburg, PA, 2013.

[7]   ACI Committee 318 Building code requirements for structural concrete (ACI 318-95) and commentary (318R-95), American Concrete Institute, Farmington Hills, Mich., 1995.

[8]   Look BG, Handbook of geotechnical investigation and design table, 1st ed. Taylor and Francis: London 2007. https://doi.org/10.1201/9780203946602

[9]   Ril 805. Guideline for load and resistance assessment of existing European railway bridges: Advices on the use of advanced methods, COWI A/S, 2007.

[10]   EN 1996-1-1: Eurocode 6: Design of masonry structures. Part 1-1: General rules for reinforced and unreinforced masonry structures, 2004.

[11]   Ersoy HY. Composite material, 1st ed. Literatür Publishing Company: Istanbul 2001. (in Turkish).

[12]   Pelà L. Aprile A. Benedetti A. Comparison of seismic assessment procedures for masonry arch bridges. Construction and Building Materials 2013; 38: 381-394. https://doi.org/10.1016/j.conbuildmat.2012.08.046

[13]   Kurtoğlu A. Material-weight relationships in wood. Journal of the Faculty of Forestry Istanbul University (in Turkish) 1983; 34(1): 150-163.

[14]   Republic of Turkey General Directorate of Highways. Technical guide for the development of design and construction technologies, Ankara (in Turkish) 2016.

[15]   Eyüpgiller KK, Ersen A, Özgen K. Irgandi Bridge restoration and reconstruction implementation, Yapı Dergisi (in Turkish) 2004; 273: 75-80.

[16]   EN 1998-1: Eurocode 8: Design of structures for earthquake resistance. Part 1: General rules, seismic actions and rules for buildings, 2005.